Cellular Physiology and Biochemistry

Cell Physiol Biochem 2018;45:2233-2245
DOI: 10.1159/000488169
Published online: March 15, 2018
Accepted: December 01, 2017

Original Paper

Molecular Insights into hERG Potassium Channel Blockade by Lubeluzole

Roberta Gualdani[a,b] Maria Maddalena Cavalluzzi[c] Francesco Tadini-Buoninsegni[a] Marino Convertino[d] Philippe Gailly[b] Anna Stary-Weinzinger[e] Giovanni Lentini[c]

[a]Dipartimento di Chimica "Ugo Schiff", Università di Firenze, Sesto Fiorentino (FI), Italy; [b]Université catholique de Louvain, Institute of Neuroscience, Laboratory of Cell Physiology, Brussels, Belgium; [c]Dipartimento di Farmacia-Scienze del Farmaco, Università degli Studi di Bari "A. Moro", Bari, Italy; [d]University of North Carolina at Chapel Hill - Department of Biochemistry and Biophysics, Chapel Hill, NC, USA; [e]Department of Pharmacology and Toxicology, University of Vienna, Vienna, Austria

Key Words
Lubeluzole • hERG channel blockers • Patch clamp • Ligand efficiency metrics

Abstract
Background/Aims: Lubeluzole is a benzothiazole derivative that has shown neuroprotective properties in preclinical models of ischemic stroke. However, clinical research on lubeluzole is now at a standstill, since lubeluzole seems to be associated with the acquired long QT syndrome and ventricular arrhythmias. Since the cardiac cellular effects of lubeluzole have not been described thus far, an explanation for the lubeluzole-induced QT interval prolongation is lacking. ***Methods:*** We tested the affinity of lubeluzole, its enantiomer, and the racemate for hERG channel using the patch-clamp technique. We synthesized and tested two simplified model compounds corresponding to two moieties included in the lubeluzole structure. The obtained experimental results were rationalized by docking simulation on the recently reported cryo-electron microscopy (cryo-EM) structure of hERG. Group efficiency analysis was performed in order to individuate the fragment most contributing to binding. ***Results:*** We found that lubeluzole and its R enantiomer are highly potent inhibitors of human ether-a-go-go-related gene (hERG) channel with an IC_{50} value of 12.9 ± 0.7 nM and 11.3 ± 0.8 nM, respectively. In the presence of lubeluzole, steady-state activation and inactivation of hERG channel were shifted to more negative potentials and inactivation kinetics was accelerated. Mutations of aromatic residues (Y652A and F656A) in the channel inner cavity significantly reduced the inhibitory effect of lubeluzole. Molecular docking simulations performed on the near atomic resolution cryo-electron microscopy structures of hERG supported the role of Y652 and F656 as the main contributors to high affinity binding. Group efficiency analysis indicated that both 1,3-benzothiazol-2-amine and 3-aryloxy-2-propanolamine moieties contribute to drug binding with the former giving higher contribution. ***Conclusions:*** This study suggests the possibility to modulate lubeluzole hERG blockade by introducing suitable substituents onto one or both constituting portions of the parent compound in order to either reduce

A. Stary-Weinzinger and G. Lentini contributed equally to this work.

Roberta Gualdani

Université catholique de Louvain, Institute of Neuroscience, Laboratory of Cell Physiology, av. Mounier 53, box B1.53.17, Brussels (Belgium)
E-Mail roberta.gualdani@uclouvain.be

potency (i. e. torsadogenic potential) or potentiate affinity (useful for class III antiarrhythmic and anticancer agent development).

Introduction

Lubeluzole [(S-1), Fig. 1A] is a benzothiazole derivative that has shown neuroprotective properties in preclinical models of ischemic stroke. The exact mechanism of neuroprotection exerted by lubeluzole, in both clinical and experimental models of cerebral ischemia [1], is not clearly defined. In fact, the drug seems to modulate *in vitro* different molecular pathways. It inhibits the signal transduction mechanisms of nitric oxide (NO) [2], the release of glutamate [3, 4], and blocks Q-type voltage-gated Ca^{2+} channels [5]. In addition, the drug blocks voltage-gated sodium channels in brain neurons and cardiomyocytes [6, 7], but it has been recently reported that its neuroprotective action is not triggered by sodium channel inhibition [8]. Since lubeluzole inhibits neuronal cyclic guanosine monophosphate (cGMP) accumulation, it has been proposed that inhibition of neuronal nitric oxide pathways may represent the main mechanism of neuroprotection [2]. The anti-ischemic activity of lubeluzole has also been related to calmodulin (CaM) activity and the counteraction of osmotic stress (mechanism associated with the release of the active amino acid taurine) [9]. The affinity of lubeluzole for CaM and its inhibiting activity on Ca^{2+}/CaM-dependent kinase II at the low micromolar level have recently been reported [10].

Moreover, lubeluzole has shown reductions of infarct volume and improved neurological function in a photothrombotic occlusion model in rats [11], and in a conventional permanent Middle Cerebral Artery Occlusion (MCAO) model also in rats [12], although the neuroprotective effects in the MCAO model were lost if administration was delayed by more than 30 minutes after onset of ischaemia. Recently, it has been demonstrated that lubeluzole synergizes with both doxorubicin and paclitaxel on human ovarian adenocarcinoma and lung carcinoma cells, respectively, over a wide concentration range (0.005-5 μM) [13]; the lowest concentration was at least 40 times lower than human plasma concentrations clinically relevant for the anti-ischemic activity [14]. In view of the above considerations, lubeluzole has been recently included in a list of sodium channel blocker candidates to repositioning [15].

Despite these promising *in vitro* and *in vivo* results, clinical research on lubeluzole is now at a standstill, since lubeluzole seems to be associated with a significant increase of heart-conduction disorders. In particular, therapeutic lubeluzole concentrations increase the action potential duration, thus causing the prolongation of the QT interval of the electrocardiogram in some of the treated patients [16, 17]. The Cochrane systematic review of lubeluzole trials [18], involving 3510 patients in five trials, confirmed lack of benefit and also significant excess risk of cardiac conduction abnormalities at all doses, including the 10 mg dose employed in most trials.

The prolongation of QT waves, caused by cardiotoxic drugs, has mainly been related to the inhibition of I_{Kr}, the current carried by the human ether-a-go-go-related gene (hERG) channel [19]. Based on this experimental evidence, as well as the finding that specific mutations in hERG are responsible for one form of congenital long-QT syndrome [20], the hERG channel assay is now considered an important antitarget in the preclinical safety testing process [21].

Since the cardiac cellular effects of lubeluzole have not been described thus far, an explanation for the lubeluzole-induced QT interval prolongation is lacking. In this article we i) tested the affinity of lubeluzole, its enantiomer, and the racemate for hERG channel using the patch-clamp technique; ii) investigated the hERG channel residues involved in the binding of lubeluzole; iii) searched for the main molecular determinants of lubeluzole block of hERG. This latter goal was pursued by designing, preparing, and testing two simplified model compounds corresponding to two moieties included in the lubeluzole structure. The obtained experimental results were rationalized by docking simulation on the recently

reported cryo-electron microscopy (cryo-EM) structure of hERG [22]. Group efficiency analysis was performed in order to identify the fragment most contributing to binding.

Materials and Methods

Chemistry

Lubeluzole [(S)-1], its R enantiomer [(R)-1], the corresponding racemate, and N-methyl-N-piperidin-4-yl-1, 3-benzothiazol-2-amine (3) (Fig. 1A) were prepared following or adapting previously reported procedures [23, 13]. Compound 3 was then converted into its hydrochloride salt by treatment with a few drops of 2 M HCl and azeotropically removing water. (S)-1-(3, 4-difluorophenoxy)-3-(piperidin-1-yl) propan-2-ol [(–)-(S)-2] (Fig. 1A) was obtained following a previously reported procedure [8].

Maintenance of mammalian cell lines and cell transfection

Patch-clamp studies were carried out on Human Embryonic Kidney (HEK) 293 cells stably transfected with hERG1a isoform, (DI.V.A.L. Toscana srl, Italy) and Chinese Hamster Ovary (CHO) cells transiently expressing hERG mutants. For heterologous protein expression, cells were plated in 6-well cell culture dishes with 2 mL growth medium, 24 h before transfection. Cells were transiently transfected with hERG mutants using TurboFect transfection reagent (Thermo Scientific). EGFP fluorescence was used as markers of successful transfection. Electrophysiology studies were performed 48/72 hr after transfection.

Electrophysiological recordings

Electrophysiological recordings were performed using the whole-cell mode of the patch-clamp technique. The extracellular solution used for patch-clamp recordings had the following composition: 140 mM NaCl, 5 mM KCl, 1 mM $MgCl_2$, 2 mM $CaCl_2$, 10 mM Glucose, 10 mM HEPES, pH 7.4 with NaOH. A modified 'high K^+' solution (containing 94 mM KCl and 50 mM NaCl) was used to study T623A and F656A hERG channel mutants [24-26]. The pipette contained: 145 mM KCl, 10 mM EGTA, 1 mM $MgCl_2$, 2 mM Mg-ATP, 10 mM HEPES, pH 7.30 with KOH. Solutions were applied to the cell via a gravity-fed perfusion system (VC-6 Six Channel Valve Controller, Warner Instruments). Patch-clamp electrodes were pulled from Sutter capillary glass (Novato, CA) on a Flaming/Brown type puller (Sutter P-87), and fire polished to 3-4 MΩ resistance, using a microforge (Narishige). To minimize voltage errors, 50–70% of the series resistance was electronically compensated. Patch-clamp recordings of cell cultures were carried out at room temperature 48h after transfection. For recordings a Multiclamp 200B amplifier (Molecular Devices, Inc, Sunnyvale, CA) and Digidata 1440 data acquisition board (Molecular Devices, Inc, Sunnydale, CA) with pCLAMP 10 software (Molecular Devices, Inc, Sunnyvale, CA) were used. Data analysis was performed using Origin 8.0 (OriginLab Corporation, Northampton, MA).

Molecular modeling

Lubeluzole was docked into the near atomic resolution cryo-EM structures of the hERG wild type (WT) (pdb: 5VA1, 3.7 Å resolution) and S631A mutant channels (pdb: 5VA3, 4.0 Å resolution) using the program Gold4.0.1 (Cambridge DataCentre, Cambridge, UK, [27]). Protein flexibility was realized including 20 snapshots derived from unbiased 500 ns all-atom Molecular Dynamics simulations (for all online suppl. material, see www.karger.com/doi/10.1159/000488169, Suppl. methods). The binding site radius was set to 20 Å around the geometric centers of Y652, which lead to a selection including all experimentally observed hERG binding determinants [20, 28, 29], as well as the hydrophobic pouches behind the selectivity filter [22]. 100, 000 operations of the GOLD genetic algorithm were used to dock both enantiomers. 100 docking poses per run were stored, with the 20 highest ranked poses analyzed in detail.

Results

Effect of lubeluzole on WT hERG

To investigate the effect of lubeluzole [(S)-1], its R enantiomer [(R)-1], and the racemic mixture (Fig. 1A) on hERG potassium channels, patch-clamp experiments were performed on HEK cells heterologously expressing the hERG channel. To elicit the activating outward

current, a depolarizing step from a holding potential of -80 mV to 0 mV (3 s in duration) was applied. Tail current was evoked by repolarizing to -40 mV for 3 s. Successive command pulses were applied at 10-second intervals.

Fig. 1B shows representative recordings of WT I_{hERG} in the absence (control) and in the presence of lubeluzole (100 nM). In the presence of lubeluzole, the tail current was strongly reduced and the I_{hERG} block induced by lubeluzole was almost irreversible, even after 10 min. of perfusion with the control solution (Fig. 1C). The inhibition caused by lubeluzole, its R enantiomer, and the racemic mixture, at each concentration, was calculated using Eq. (1) (see online suppl. material) and the mean values, after normalization, were plotted as shown in Fig. 1D. Fitting the data in Fig. 1D with the Hill equation [Eq. (2), (see online suppl. material)] yielded an IC_{50} of 12.9 ± 0.7 nM and a Hill slope (nH) of 0.84 ± 0.05, for lubeluzole; an IC_{50} of 11.3 ± 0.8 nM and a nH of 0.79 ± 0.04 for its R enantiomer; an IC_{50} of 11.1 ± 0.4 nM and a nH of 1.1 ± 0.03 for the racemic mixture (Fig. 1D). Since no statistically significant differences between IC_{50} values were obtained, we conclude that lubeluzole binds hERG channel in a non-stereoselective manner.

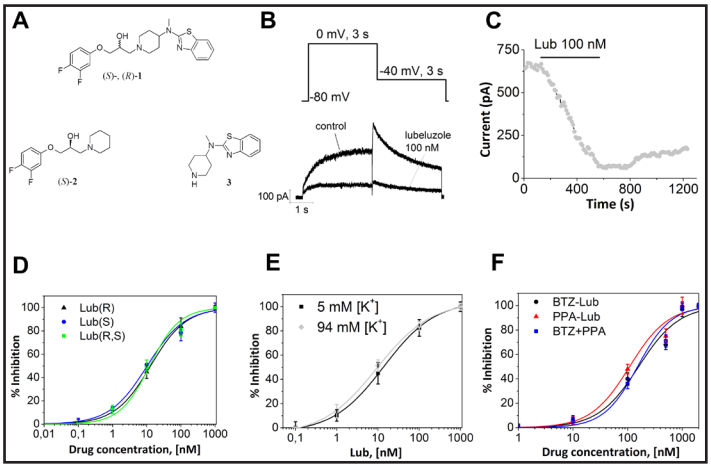

Fig. 1. A) Structures of lubeluzole and its simplified analogues. B) Pulse protocol and representative hERG currents obtained before (control) and after addition of 100 nM of lubeluzole. C) Time course of lubeluzole-induced hERG tail current inhibition from the same cell shown in (B). D) Concentration-response relationship (mean ± SEM) for block of hERG tail current by lubeluzole, its R enantiomer, and the racemic mixture (n = 5 per data point). E) Concentration response relationships obtained from inward I_{hERG}, in the presence of lubeluzole, using 'normal' [K^+] (5 mM) and 'high' [K^+] (94 mM) solutions. F) Concentration-response relationship (mean ± SEM) for block of hERG tail current by BTZ-lub, PPA-lub and BTZ-lub+PPA-lub (n = 5 per data point).

Due to the known low expression and altered kinetic properties of some hERG mutants (in particular T623A and F656A clones), we measured the inward current of the T623A and F656A mutants in high (94 mM) external K^+ solution, since the external K^+ concentration increase is aimed to maximize the inward tail currents [25, 26, 30]. Consequently, we tested lubeluzole block of wild-type I_{hERG} under similar experimental conditions, to examine whether a change in the ionic conditions affects hERG affinity toward lubeluzole. Fig. 1E shows the concentration response relationships obtained from inward I_{hERG} elicited at -120 mV using 'normal' [K^+] (5 mM) and 'high' [K^+] (94 mM) solutions. From the experimental data in Fig. 1E we obtained an IC_{50} of 13 ± 4 nM and a nH of 0.70 ± 0.06 for the inward I_{hERG} in 'normal' [K^+] solution, and an IC_{50} of 10.4 ± 1.4 nM and a nH of 0.66 ± 0.07 for the inward I_{hERG} in 'high' [K^+] solution. Since these values are similar to those found from the concentration-response relationship of hERG outward current inhibition by lubeluzole, we conclude that lubeluzole-induced block of I_{hERG} is not influenced by the concentration or the direction of flux of K^+ ions, as in the case of other hERG channel blockers (e.g. flecainide [31]).

Effect of lubeluzole moieties on WT hERG channels

Structurally, lubeluzole contains two portions: an aryloxypropranolamine moiety, recalling β-adrenergic blockers like propranolol [compound (S)-2, Fig. 1A] and a 1, 3-benzothiazol-2-amine moiety related to riluzole (compound 3, Fig. 1A). Both riluzole

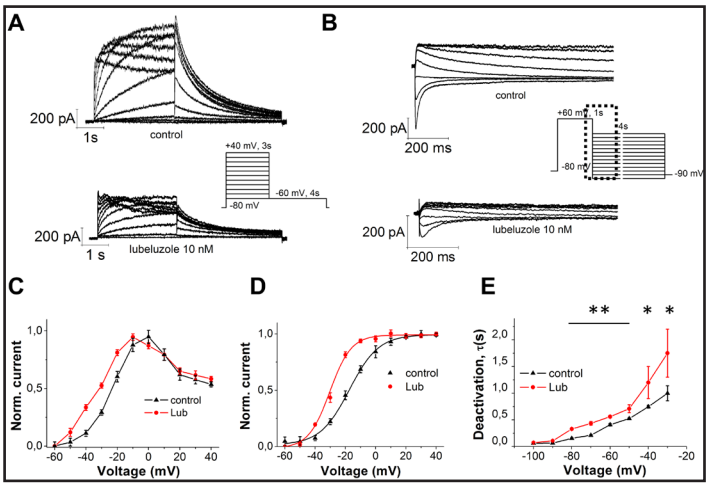

Fig. 2. A) Pulse protocol and representative hERG current traces, in the absence (control) or presence of 10 nM lubeluzole. B) Representative hERG current traces elicited by the voltage protocol shown in the middle panel, testing deactivation currents, in the absence (control) or presence of 10 nM lubeluzole. Current traces before and after application of lubeluzole are depicted on an expanded time scale (marked as dotted squares in the pulse protocol). C) Normalized (with respect to the control currents) I-V relationships for activation current measured during the depolarizing steps, before (control) and after addition (time of incubation ≥ 10 min) of 10 nM lubeluzole. Error bars for some points are masked by symbols (n ≥ 5 cells per data-point). D) Normalized (with respect to the control currents) I-V relationships for current measured at the tail current peaks, before (control) and after addition (time of incubation ≥ 10 min) of 10 nM lubeluzole. Error bars for some points are masked by symbols (n ≥ 5 cells per data-point). I-V relationships for tail current amplitudes were fitted with a Boltzmann function. $V_{1/2}$ shifted from -16 ± 3 mV (control), to -24 ± 1 mV (P<0.001, paired t-test). E) Time constants of deactivation current acquired using the protocol shown in (B). Time constants (τ) of deactivation were obtained from monoexponential fits to the decay of tail currents during the 4s- voltage step to various potentials. Data are expressed as mean ± SEM (n ≥ 5 per data point). ** P<0.01, *P<0.05 (Two way ANOVA followed by Bonferroni test).

and propranolol are potent sodium channel blockers. Block of sodium channels caused by riluzole seems to be involved in the efficacy of the drug in amyotrophic lateral sclerosis [32]. Propranolol blocks sodium channels in a similar manner to local anesthetics [33]. In view of their pharmacological properties, we decided to analyze in detail the effects of the two lubeluzole moieties on hERG channels expressed in HEK cells.

The aryloxypropranolamine (PPA-lub) and 1,3-benzothiazol-2-amine (BTZ-lub) moieties were analyzed individually or mixed together and their effects on hERG currents are reported in Fig. 1F. Our data show that the IC_{50} value of lubeluzole is one order of magnitude lower than those of the two moieties, i.e. IC_{50} = 160 ± 12 nM and nH = 1.17 ± 0.22 (BTZ-lub), IC_{50} = 109 ± 16 nM and nH = 1.22 ± 0.19 (PPA-lub), and IC_{50} = 152 ± 11 nM and nH = 1.40 ± 0.28 (BTZ-lub + PPA-lub). This suggests that lubeluzole binds more effectively to hERG channel with respect to the two moieties, acting individually or mixed in the same solution.

Effect of lubeluzole on hERG activation and deactivation

The voltage-dependence of lubeluzole-induced inhibition was measured on hERG K^+ current amplitudes, applying the protocol shown in Fig. 2A. Tail currents were elicited by repolarization to -60 mV. Individual tail current amplitudes recorded before (control) or after addition of 10 nM lubeluzole, were normalized to the maximal control amplitude and fitted with a Boltzmann function (Fig. 2B). The presence of lubeluzole caused a left-shift by -10 mV of the I-V relationship of hERG activation current (Fig. 2C). Moreover, the voltage required for half-maximal activation ($V_{1/2}$) was leftwards shifted in the presence of lubeluzole, from -16 ± 3 mV (control) to -24 ± 1 mV (lubeluzole) (Fig. 2D). Since the $V_{1/2}$ value of hERG channels is shifted to more negative potentials in the presence of lubeluzole, we conclude that the drug might affect the activation gating of the channel.

Deactivation time constants were obtained by fitting with a single exponential function the currents recorded using the protocol shown in Fig. 2B. As shown in Fig. 2E, lubeluzole slightly increases the deactivation time constant.

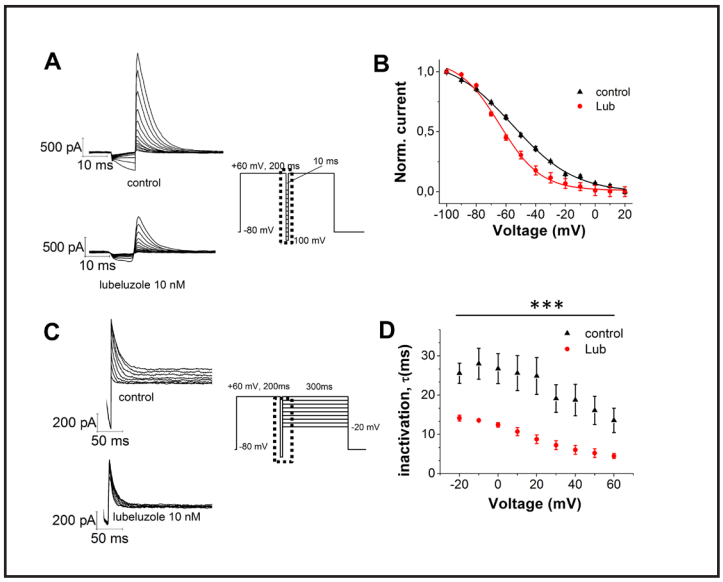

Fig. 3. hERG channel inactivation. A) Representative hERG current traces, in the absence (control) or presence of 10 nM lubeluzole, elicited by the voltage protocol shown in the middle panel, testing steady-state inactivation currents. B) Normalized steady-state I-V inactivation curves before (control) and after application of 10 nM lubeluzole. Data are expressed as mean ± SEM; error bars for some points are masked by symbols. Solid lines represent fits with Boltzmann function. $V_{1/2}$ shifted from -55 ± 1 mV (control), to -70 ± 1 mV (P<0.001, paired t-test; n = 6 cells). Currents traces before and after application of lubeluzole are depicted on an expanded time scale (marked as dotted squares in the pulse protocol). C) Pulse protocol and representative onset of inactivation currents, in the absence (control) or presence of 10 nM lubeluzole. D) Inactivation time constants were derived from currents acquired using the protocol shown in (C), fitted with a single exponential function to the decay of tail currents during the third 300-ms voltage step, and plotted against the membrane potential. Data are expressed as mean ± SEM (n ≥ 5 per data point). ***P<0.001 (Two way ANOVA followed by Bonferroni test).

Relationship between lubeluzole block and hERG channel inactivation

I_{hERG} inhibition by drugs can be influenced (or not) by channel inactivation [34- 37, 25].

Steady-state inactivation currents were measured following the three-step protocol reported in Fig. 3A: channels were inactivated at +60 mV, before short test pulses from -100 mV to +20 mV were applied, to recover the channels from inactivation. Depolarization to +60 mV after these test pulses evoked a large outward inactivating current. Fig. 3A shows sample traces of inactivating current I_{hERG} in the absence (control) and in the presence of 10 nM lubeluzole. Current amplitudes measured after depolarization to +60 mV were normalized, plotted against the corresponding test voltage and fitted by a Boltzmann function (Eq. (3), see online suppl. material). Our data indicate that lubeluzole causes a leftward shift in $V_{1/2}$ values of steady-state inactivation, from -55 ± 1 mV in the absence of the drug (control) to -70 ± 1 mV in the presence of lubeluzole (Fig. 3B).

The effect of lubeluzole on the inactivation time course was also investigated using the protocol shown in Fig. 3C. From a holding potential of -80 mV, a 200 ms test pulse to +60 mV was applied to inactivate the channel. Moreover, a short pulse to -100 mV and voltage steps from -20 mV to +60 mV (300 ms, 10 mV-increments) were applied to elicit a large outward inactivating current. Fig. 3C shows sample traces of inactivating current I_{hERG} in the absence or presence of 10 nM lubeluzole. Inactivation currents were fitted by a single exponential function to extrapolate time constant values. Fig. 3D shows that the inactivation kinetics of hERG channel is significantly accelerated in the presence of lubeluzole.

Effect of mutations in the hERG pore helix and inner cavity on lubeluzole potency

A cluster of three residues (T623, S624 and V625) located in the lower portion of the pore helix-selectivity filter region has been reported to be involved in the binding of different drugs to hERG [20, 28]. Moreover, it was shown that hERG channel blockers are able to bind within the channel inner cavity, interacting with one or two aromatic residues of the S6 domain (Tyr652 and Phe656) [38]. In order to determine the roles of these residues

in lubeluzole block of I_{hERG}, we studied the alanine mutants, S624A, V625A and Y652A, under 'normal' [K^+] solution. The current associated with these mutants was elicited by the standard voltage protocol shown in Fig. 1B (Fig. 4A). The T623A and F656A mutants were tested under 'high' [K^+] solution and the current was elicited by a hyperpolarizing step to -120 mV in order to obtain an appreciable inward current transient. Representative traces of T623A and F656A currents in the absence (control) and in the presence of 10 nM lubeluzole are shown in Fig. 4B. Different lubeluzole concentrations were tested and a full concentration–response relationship was constructed for each mutant, as shown in Fig. 4C and 4D. The corresponding IC_{50} values are summarized in Fig. 4E and Table 1, indicating that the two aromatic residues F656 and Y652 have a prominent role in lubeluzole block of I_{hERG}.

Binding modes of lubeluzole to different hERG channel states

Lubeluzole interactions with the hERG channel in a putative open inactivated (WT cryo-EM structure) and an open activated state (S631A mutant structure) were analyzed performing docking calculations. A close-up view of the predicted drug-binding interactions is shown in Fig. 5 (WT) and Fig. 6 (S631A). In agreement with mutagenesis data (Fig. 4), π-π interactions between the benzothiazole ring and the aromatic moiety of the Y652 side chains were observed in the large majority (> 95%) of all docking poses obtained for both WT and S631A channels. Hydrophobic and π-π interactions were frequently observed between the difluorophenoxy ring of lubeluzole and the Y652 and F656 side chains. The protonatable nitrogen is located at the center of the strong electronegative cavity, but no cation-π interactions were observed in any of the docking poses. Hydrogen bonds to residues at the base of the selectivity filter (T623, S624) are not observed, in agreement with the very moderate effects of the respective alanine mutants (Fig. 4E). No differences between the two enantiomers were seen (data not shown). Generally, the high affinity of the compound in the relative narrow hERG cavities is achieved, via maximizing favorable π-π and hydrophobic contacts with Y652 and F656 and lubeluzole.

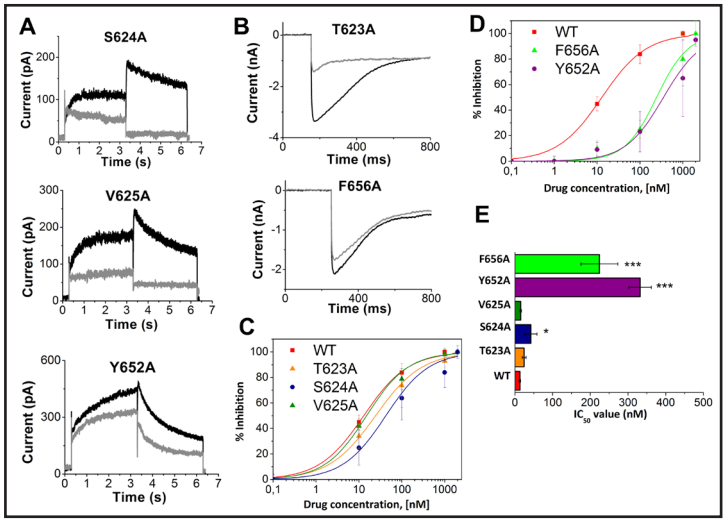

Fig. 4. A) Representative I_{hERG} traces of S624A, V625A and Y652A mutants in the absence (black line) and presence (grey line) of 100 nM lubeluzole. The tail current was evoked by repolarization from 0 to -50 mV (same protocol shown in the lower panel of Fig.1B) and was recorded under the 'normal' external solution ([K^+] = 5 mM). B) Representative I_{hERG} traces of T623A and F656A mutants in the absence (black line) and presence (grey line) of 100 nM lubeluzole. The tail current was evoked by repolarization from +20 to -120 mV (protocol shown (see online suppl. material) in Fig. S1) and was recorded using 'high' [K^+] solution (94 mM). C) Concentration-response relationships for current of T623A, S624A, V625A mutants blocked by lubeluzole. Each value represents mean ± SEM of n ≥ 5 cells. D) Concentration-response relationships for Y652A and F656A mutants. Each value represents mean ± SEM of n ≥ 5 cells. E) IC_{50} values for lubeluzole inhibition of the alanine mutants shown in (A) and (B), compared with WT-hERG. Each IC_{50} was obtained from a concentration–response relationship derived from at least four different drug concentrations. ***P<0.001, *P<0.05 (paired t-test); n ≥ 5 for each concentration on each curve.

Discussion

Lubeluzole is a benzothiazole derivative that has shown neuroprotective properties in preclinical models of ischemic stroke. However, clinical research on lubeluzole is now at a standstill, since lubeluzole seems to be associated with the acquired long QT syndrome and ventricular arrhythmias.

Our data showed that lubeluzole and its R enantiomer are highly potent inhibitors of hERG current with an IC_{50} value of 12.9 ± 0.7 nM and 11.3 ± 0.8 nM, respectively. In the presence of lubeluzole steady-state activation and inactivation of hERG channel were shifted to more negative potentials and inactivation kinetics was accelerated. Mutations of aromatic residues (Y652A and F656A) in the channel inner cavity significantly reduced the inhibitory effect of lubeluzole.

Table 1. Parameters (IC_{50}, n_H) derived from the Hill fit of the concentration-response relationships of inhibition of hERG channels (WT, T623A, S624A, V625A, Y652A, F656A) by lubeluzole and its moieties. For all channel variants, the direction of I_{hERG} and the external K^+ concentration were specified in brackets

hERG gene	Compound	IC_{50}	n_H
WT (out. 5 mM K^+)	Lub(S)	12.9 ± 0.7 nM	0.84 ± 0.05
WT (inw. 94 mM K^+)	Lub(S)	10.4 ± 1.4 nM	0.66 ± 0.07
WT (out. 5 mM K^+)	Lub(R)	11.3 ± 0.8 nM	0.79 ± 0.04
WT (out. 5 mM K^+)	Lub(R,S)	11.1 ± 0.4 nM	1.10 ± 0.03
WT (out. 5 mM K^+)	BTZ-Lub	160 ± 12 nM	1.17 ± 0.22
WT (out. 5 mM K^+)	PPA-Lub	109 ± 16 nM	1.22 ± 0.19
WT (out. 5 mM K^+)	BTZ-Lub+PPA-Lub	152 ± 11 nM	1.40 ± 0.28
T623A (inw. 94 mM K^+)	Lub(S)	24 ± 5.0 nM	0.80 ± 0.09
S624A (out. 5 mM K^+)	Lub(S)	42 ± 16 nM	1.17 ± 0.22
V625A (out. 5 mM K^+)	Lub(S)	15.4 ± 2.1 nM	0.89 ± 0.11
Y652A (out. 5 mM K^+)	Lub(S)	350 ± 40 nM	0.98 ± 0.19
F656A (inw. 94 mM K^+)	Lub(S)	240 ± 50 nM	1.17 ± 0.19

Examination of the binding modes obtained from docking calculations suggests that lubeluzole binds to the central cavity of the hERG channel and π-π and hydrophobic interactions with Y652 and F656 are the main contributors to high affinity binding of this drug.

The recently solved hERG cryo-EM structures at near atomic resolution revealed the existence of hydrophobic pouches protruding from the cavity towards the extracellular side, and a possible role for drug-binding was suggested [22]. However, at least for lubeluzole these regions do not seem to contribute to drug-binding. Only in < 5% of the docking poses the difluorphenoxy moiety of lubeluzole partially protruded into one such hydrophobic pocket. No clear state-dependent changes could be observed, when comparing the WT and S631A docking poses, which might be due to the subtle structural differences and the general low resolution of the structures (3.7 Å and 4 Å).

The presence of low stereoselectivity in hERG blockers is a generally observed feature [40] and may be explained invoking both the plasticity and symmetry of the channel [41]. However, eudismic analysis on bupivacaine enantiomers recently unravelled moderate stereoselectivity (stereoselectivity index, SSI = IC_{50}distomer/IC_{50}eutomer ~ 7) [42]. While blocking hERG with 1000-fold higher potency than bupivacaine, lubeluzole and its enantiomer displayed no stereoselectivity at all (SSI = 0) thus conflicting with the Pfeiffer's rule [43]. However, the following considerations may help explain the complete lack of stereoselectivity observed in our work (for the sake of simplicity, the discussion will be focused on lubeluzole while all considerations obviously hold for its enantiomer too).

First of all, lubeluzole is at least ten times less basic than bupivacaine, with pK_a values being 7.14 [8] and 8.17 [44] for lubeluzole and bupivacaine, respectively. Moreover, the protonatable nitrogen of lubeluzole is displaced by one carbon atom from the stereogenic center, unlike bupivacaine, in which the protonatable nitrogen is closer to the stereogenic

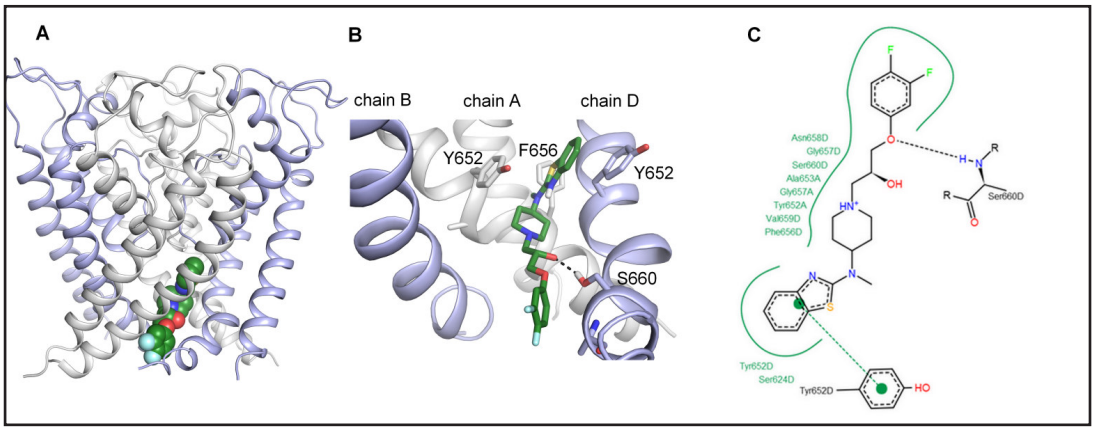

Fig. 5. A) Lubeluzole bound to the WT hERG cryo-EM structure. B) Details of the highest scoring binding pose of lubeluzole shown in sticks representation. Hydrogen bonds are depicted as black dotted lines. C) 2D interaction profiles were generated with PoseView [39]. Green dotted lines indicate π-π interactions between aromatic rings; green solid lines represent hydrophobic interactions. Hydrogen bonds are shown as black dotted lines.

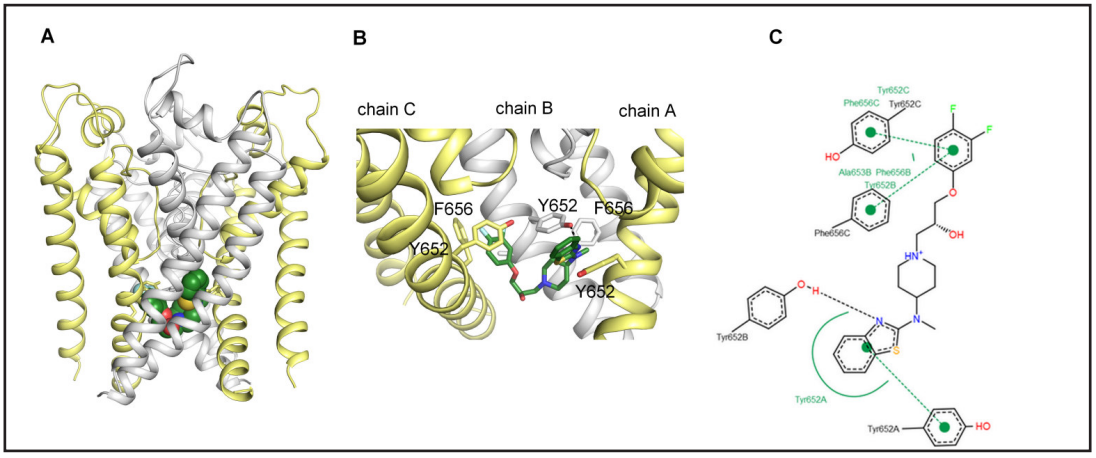

Fig. 6. A) Lubeluzole bound to the S631A mutant structure. B) Details of the highest scoring binding pose of lubeluzole shown in sticks representation. Hydrogen bonds are depicted as black dotted lines. C) 2D interaction profiles were generated with PoseView [39]. Green dotted lines indicate π-π interactions between aromatic rings; green solid lines represent hydrophobic interactions. Hydrogen bonds are shown as black dotted lines.

center. This consideration could explain why the contribution of the basic group to stereoselective binding should be relatively less important in lubeluzole than in bupivacaine. On the other hand, our modeling experiments showed no cation-π interactions in any docking pose.

Secondly, lubeluzole is a relatively flexible compound and its protonatable nitrogen is symmetrically substituted. Thus, even occurring, protonation would not add chiral stereoelectronic demand.

Finally, lubeluzole has a relatively symmetric structure roughly depictable as being constituted by two planar portions spaced by an aliphatic linker. The latter, in turn, bears two possibly less relevant pharmacophoric elements, the hydroxyl group and the partially protonated nitrogen atom. Chirality is conferred by the carbinolic group which bears two methylene groups separating the bulkiest molecular moieties. Thus, it may be assumed that the stereogenic requirements imposed by the chirality center are mitigated by the

fact that the two bulkiest portions of the molecule are symmetrically spaced by two, freely rotating methylene groups.

The potency of hERG blocking agents is generally related to MW and lipophilicity, with amines being the most redoubtable drugs [45]. It comes as no surprise that lubeluzole (MW = 434 Da, cLog *P* = 4.7) was at least 10 thousand times more potent than its constituting fragments PPA-lub (MW = 271 Da, cLog *P* = 3.2) and BTZ-lub (MW = 247 Da, cLog *P* = 2.4) (Fig. 7). Less predictable was the light rise in ligand efficiency (LE = 1.37pIC$_{50}$/HA [46]) observed when passing from the two fragments PPA-lub (LE = 0.21) and BTZ-lub (LE = 0.22) to lubeluzole (LE = 0.26) while generally the contrary is found throughout drug-like molecule space: a decrease in LE is commonly observed with increasing MW [46]. Roughly speaking, this means that the non-hydrogen atoms (HA) constituting the two fragments contribute more efficiently to the binding when the two moieties are linked together to give lubeluzole structure than when acting individually. In fact, lubeluzole presented the highest lipophilic ligand efficiency (LLE = pIC$_{50}$ – cLog *P*) [47] value (3.2, Fig. 7), thus indicating that it is the most specific ligand out of the three. In other words, the increase in potency observed when passing from the two fragments to lubeluzole was not merely due to increased lipophilicity. However, both LE and LLE values were relatively low, thus indicating that the driving force of lubeluzole blocking activity is mostly entropic (i. e, sustained by van der Waals and hydrophobic contributions [48]). The last statement is in agreement with the observed null stereoselectivity and docking results.

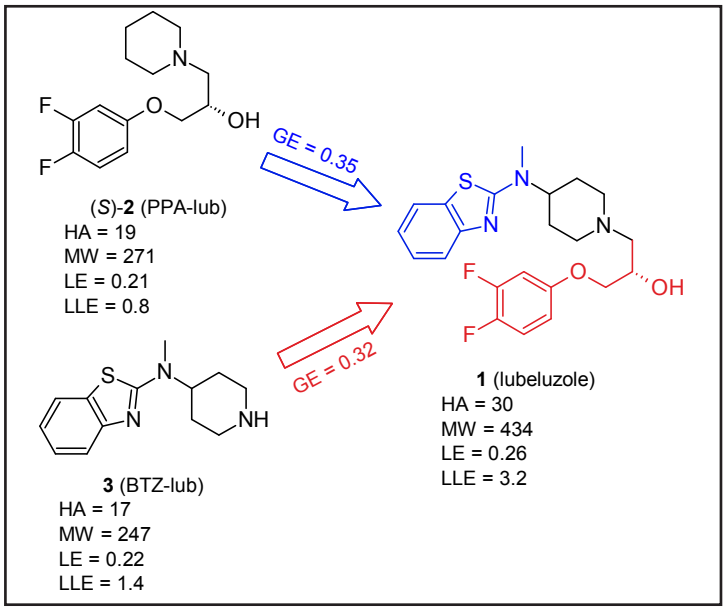

Fig. 7. Ligand efficiency metric analysis. Group efficiency: GE = ΔΔG/Δnumber of non-hydrogen atoms = Δ1.37pIC$_{50}$/ΔHA [48]; ligand efficiency: LE = 1.37pIC$_{50}$/HA [45]; lipophilic ligand efficiency: LLE = pIC$_{50}$ – cLog P [46].

When group efficiency (GE = ΔΔG/Δnumber of non-hydrogen atoms = Δ1.37pIC$_{50}$/ΔHA) [49, 50] is considered, the 2-aminobenzothiazolic moiety emerged as the most interesting portion (GE = 0.35) since its contribution to lubeluzole potency of block is higher than the one granted by the 3-aryloxy-2-hydroxypropyl portion (GE = 0.32).

Conclusion

Both moieties of lubeluzole contribute to binding. Suitable substituents may be introduced onto both moieties to allow modulation of hERG blocking activity. The benzothiazole ring should be given priority in structure-activity relationship studies.

The interaction of drugs with hERG is generally feared as a source of toxicological concern due to torsadogenic (i. e. proarrhythmic) potential. In this respect, we propose that the introduction of suitable substituents on one or both constituting portions of lubeluzole structure might be exploited to reduce hERG affinity. On the other hand, a therapeutic potential has been suggested for hERG blockers as class III antiarrhythmic and anticancer agents [51]. In this respect, our study let envisage the possibility to develop new lubeluzole

analogues possibly endowed with more convenient pharmacological profile through both classical structure-activity relationships and computer-assisted studies.

Acknowledgements

We would like to thank Prof. Doug Golenbock (University of Massachusetts Medical School, Boston, USA) for providing pcDNA3-EGFP (Addgene plasmid 13031); Dr. Aziza El Harchi (School of Physiology & Pharmacology, Faculty of Biomedical Sciences, University of Bristol) and Dr. X. Koenig (Medical University of Vienna) for providing hERG mutant plasmids. The computational results presented have been achieved using the Vienna Scientific Cluster (VSC). This work was supported by the Austrian Science Fund (FWF), grant nr. W1232 to A.S.W.

Disclosure Statement

No conflict of interests exists.

References

1 De Ryck M, Keersmaekers R, Duytschaever H, Claes C, Clincke G, Janssen M, Van Reet G: Lubeluzole protects sensorimotor function and reduces infarct size in a photochemical stroke model in rats. J Pharmacol Exp Ther 1996;279:748-758.
2 Maiese K, TenBroeke M, Kue I: Neuroprotection of lubeluzole is mediated through the signal transduction pathways of nitric oxide. J Neurochem 1997;68:710-714.
3 Lesage AS, Peeters L, Leysen JE: Lubeluzole, a novel long-term neuroprotectant, inhibits the glutamate-activated nitric oxide synthase pathway. J Pharmacol Exp Ther 1996;279:759-766.
4 Scheller D, Kolb J, Szathmary S, Zacharias E, De Ryck M, Van Reempts J, Clincke G, Tegtmeier F: Extracellular changes of gluta-mate in the periinfarct zone: effect of lubeluzole. J Cereb Blood Flow Metab 1995;15:S379.
5 Marrannes R, De Prins E, Clincke G: Influence of lubeluzole on voltage-sensitive Ca^{2+} channels in isolated rat neurons. J Pharmacol Exp Ther 1998;286:201–214.
6 Osikowska-Evers BA, Wilhelm D, Nebel P, Hennemann E, Scheufler E, Tegtmeier F: The effects of the novel neuroprotective compound lubeluzole on sodium current and veratridine induced sodium load in rat brain neurons and synaptosomes. J Cereb Blood Flow Metab 1995;15:380S.
7 Le Grand B, Talmant JM, Rieu JP, Patoiseau JF, John GW: Study of the interaction of lubeluzole with cardiac sodium channels. J Cardiovasc Pharmacol 2003;42:581-587.
8 Desaphy JF, Carbonara R, Costanza T, Lentini G, Cavalluzzi M.M, Bruno C, Franchini C, Conte Camerino D: Molecular dissection of lubeluzole use-dependent block of voltage-gated sodium channels discloses new therapeutic potentials. Mol Pharmacol 2013;83:406-415.
9 Zielińska M, Hilgier W, Borkowska HD, Oja SS, Saransaari P, Albrecht J: Lubeluzole attenuates K(+)-evoked extracellular accumulation of taurine in the striatum of healthy rats and rats with hepatic failure. Brain Res 2001;904:173-176.
10 Bruno C, Cavalluzzi MM, Rusciano MR, Lovece A, Carrieri A, Pracella R, Giannuzzi G, Polimeno L, Viale M, Illario M, Franchini C, Lentini G: The chemosensitizing agent lubeluzole binds calmodulin and inhibits Ca(2+)/calmodulin-dependent kinase II. Eur J Med Chem 2016;116:36-45.
11 De Ryck M, Verhoye M, Van der Linden AM: Diffusion-weighted MRI of infarct growth in a rat photochemical stroke model: effect of lubeluzole. Neuropharmacology 2000;39:691-702.
12 Aronowski J, Strong R, Grotta JC: Treatment of experimental focal ischemia in rats with lubeluzole. Neuropharmacology 1996;35:689-693.
13 Cavalluzzi MM, Viale M, Bruno C, Carocci A, Catalano A, Carrieri A, Franchini C, Lentini G: A convenient synthesis of lubeluzole and its enantiomer: evaluation as chemosensitizing agents on human ovarian adenocarcinoma and lung carcinoma cells. Bioorg Med Chem Lett 2013;23:4820-4823.

14 Diener HC, Hacke W, Hennerici M, Rådberg J, Hantson L, De Keyser J: Lubeluzole in acute ischemic stroke. A double-blind, placebo-controlled phase II trial. Lubeluzole International Study Group. Stroke 1996;27:76-81.
15 Gualdani R, Cavalluzzi M. M, Lentini G: Recent Trends in the Discovery of Small Molecule Blockers of Sodium Channels. Curr Med Chem 2016;23:2289-2332.
16 Sugiyama A, Ni C, Arita J, Eto K, Xue YX, Hashimoto K: Effects of the antihypoxic and neuroprotective drug, lubeluzole, on repolarization phase of canine heart assessed by monophasic action potential recording. Toxicol Appl Pharmacol 1996;139:109-114.
17 Le Grand B, Dordain-Maffre M, John GW: Lubeluzole-induced prolongation of cardiac action potential in rabbit Purkinje fibres. Fundam Clin Pharmacol 2000;14:159-162.
18 Gandolfo C, Sandercock P, Conti M: Lubeluzole for acute ischaemic stroke. Cochrane Database Syst Rev 2002;1:CD001924.
19 Sanguinetti MC, Curran ME, Zou A, Shen J, Spector PS, Atkinson DL, Keating MT: Coassembly of K(V)LQT1 and minK (IsK) proteins to form cardiac I(Ks) potassium channel. Nature 1996;384: 80–83.
20 Mitcheson JS, Chen J, Lin M, Culberson C, Sanguinetti MC: A structural basis for drug-induced long QT syndrome. Proc Natl Acad Sci U S A 2000;97:12329–12333.
21 Food and Drug Administration, HHS. International Conference on Harmonisation;guidance on S7B Nonclinical Evaluation of the Potential for Delayed Ventricular Repolarization (QT Interval Prolongation) by Human Pharmaceuticals; availability. Notice. Fed Regist 2005;70:611336-1134.
22 Wang W, MacKinnon R: Cryo-EM Structure of the Open Human Ether-à-Go-Go-Related K^+ Channel hERG. Cell 2017;169:422–430.
23 Bruno C, Carocci A, Catalano A, Cavalluzzi MM, Corbo F, Franchini C, Lentini G, Tortorella V: Facile, alternative route to lubeluzole, its enantiomer, and the racemate. Chirality 2006;18:227–231.
24 Sanguinetti MC, Chen J, Fernandez D, Kamiya K, Mitcheson J, Sanchez Chapula JA: Physicochemical basis for binding and voltage-dependent block of hERG channels by structurally diverse drugs. Novartis Found Symp 2005;266:159–166.
25 El Harchi A, Zhang YH, Hussein L, Dempsey CE, Hancox JC: Molecular determinants of hERG potassium channel inhibition by disopyramide. J Mol Cell Cardiol 2012;52:185–195.
26 Du C, Zhang Y, El Harchi A, Dempsey CE, Hancox JC: Ranolazine inhibition of hERG potassium channels: drug-pore interactions and reduced potency against inactivation mutants. J Mol Cell Cardiol 2014;74:220–230.
27 Jones G, Willett P, Glen RC: Molecular recognition of receptor sites using a genetic lgorithm with a description of desolvation. J Mol Biol 1995;245:43–53. GOLD, version 4.0; Cambridge Crystallographic Data Centre: Cambridge, U.K. GOLD, version 4.0; Cambridge Crystallographic Data Centre: Cambridge, U.K.
28 Kamiya K, Niwa R, Mitcheson JS, Sanguinetti MC: Molecular determinants of hERG channel block. Mol Pharmacol 2006;69:1709–1716.
29 Saxena P, Zangerl-Plessl EM, Linder T, Windisch A, Hohaus A, Timin E, Hering S, Stary-Weinzinger A: New potential binding determinant for hERG channel inhibitors. Sci Rep 2016;6:24182.
30 Zhang Y, Colenso CK, El Harchi A, Cheng H, Witchel HJ, Dempsey CE, Hancox JC: Interactions between amiodarone and the hERG potassium channel pore determined with mutagenesis and in silico docking. Biochem Pharmacol 2016;113:24–35.
31 Melgari D, Zhang Y, El Harchi A, Dempsey CE, Hancox JC: Molecular basis of hERG potassium channel blockade by the class Ic antiarrhythmic flecainide. J Mol Cell Cardiol 2015;86:42–53.
32 Wang YJ, Lin MW, Lin AA, Wu SN: Riluzole-induced block of voltage-gated Na^+ current and activation of BKCa channels in cultured differentiated human skeletal muscle cells. Life Sci 2008;82:1120.
33 Wang DW, Mistry AM, Kahlig KM, Kearney JA, Xiang J, George Jr AL: Propranolol blocks cardiac and neuronal voltage-gated sodium channels. Front Pharmacol 2010;1:144.
34 Lees-Miller JP, Duan Y, Teng GQ, Duff HJ: Molecular determinant of high-affinity dofetilide binding to HERG1 expressed in Xenopus oocytes: involvement of S6 sites. Mol Pharmacol 2000;57:367–374.
35 McPate MJ, Duncan RS, Hancox JC, Witchel HJ: Pharmacology of the short QT syndrome N588K-hERG K^+ channel mutation: differential impact on selected class I and class III antiarrhythmic drugs. Br J Pharmacol 2008;155:957–966.

36 Ficker E, Jarolimek W, Brown AM: Molecular determinants of inactivation and dofetilide block in ether a-go-go (EAG) channels and EAG-related K (+) channels. Mol Pharmacol 2001;60:1343–1348.
37 Perrin MJ, Kuchel PW, Campbell TJ, Vandenberg JI: Drug binding to the inactivated state is necessary but not sufficient for high-affinity binding to human ether-à-go-go-related gene channels. Mol Pharmacol 2008;74:1443–1452.
38 Sanguinetti MC, Mitcheson JS: Predicting drug-hERG channel interactions that cause acquired long QT syndrome. Trends Pharmacol Sci 2005;26:119–124.
39 Poseview. Stierand K, Maaß P, Rarey M: Molecular Complexes at a Glance: Automated Generation of two-dimensional Complex Diagrams. Bioinformatics 2006;22:1710-1716.
40 Grilo LS, Carrupt P-A, Abriel H: Stereoselective Inhibition of the hERG1 Potassium Channel. Front Pharmacol 2010;1:137.
41 Dempsey CE, Wright D, Colenso CK, Sessions RB, Hancox JC: Assessing hERG pore models as templates for drug docking using published experimental constraints: the inactivated state in the context of drug block. J Chem Inf Model 2014;54:601–612.
42 Grilo LS, Carrupt P-A, Abriel H, Daina A: Block of the hERG channel by bupivacaine: electrophysiological and modelling insights towards stereochemical optimization. Eur J Med Chem 2011;46:3486-3498.
43 Pfeiffer CC: Optical isomerism and pharmacological action, a generalisation. Science 1956;124:29–31
44 Kamaya H, Hayes JJ, Ueda I: Dissociation constants of local anesthetics and their temperature dependence. Anesth Analg 1983;62:1025-1230.
45 Gleeson MP: Generation of a set of simple, interpretable ADMET rules of thumb. J Med Chem 2008;51:817–834.
46 Hopkins AL, Groom CR, Alex A: Ligand efficiency: a useful metric for lead selection. Drug Discov Today 2004;9:430-431.
47 Leeson PD, Springthorpe B: The influence of drug-like concepts on decision-making in medicinal chemistry. Nat Rev Drug Discov 2007;6:881–890.
48 Kuntz ID, Chen K, Sharp KA, Kollman, PA: The maximal affinity of ligands. Proc Natl Acad Sci U S A 1999;96:9997-10002.
49 Verdonk ML, Rees DC: Group Efficiency: A Guideline for Hits-to-Leads Chemistry. ChemMedChem 2008;3:1179–1180.
50 Cavalluzzi MM, Mangiatordi GF, Nicolotti O, Lentini G: Ligand Efficiency Metrics in Drug Discovery: the Pros and Cons from a Practical Perspective. Exp Opin Drug Discov 2017;12:1087-1104.
51 Arcangeli A, Becchetti A: hERG Channels: From Antitargets to Novel Targets for Cancer Therapy. Clin Cancer Res 2017;23:3–5.